Article ID: 1000-7032(2019)04-0459-09

Growth Mechanism of TiO_2 Nanotube Arrays by Etching Treatment and Their Photoelectric Property

SUN Qiong[1,2*], YOU Di[1], ZANG Tao[1],
WU Song-hao[1], HONG Yong[1], DONG Li-feng[1]

(1. *College of Materials Science and Engineering, Qingdao University of Science and Technology, Qingdao* 266042, *China*;
2. *State Key Laboratory of Photocatalysis on Energy and Environment, Fuzhou University, Fuzhou* 350116, *China*)

* *Corresponding Author, E-mail: sunqiong@qust.edu.cn*

Abstract: In this research, densely aligned TiO_2 nanorods are etched into nanotubes by hydrochloric acid, and the growth mechanism is also supposed. During the etching process, the dents appear from the top down and inside out along the growth direction of the nanorod, and finally form the tube structure. Actually, the nanotube with square hollow cross section consists of a mass of surrounded fine nanowires, which will be teared into independent ones at high temperature. When assembled into dye sensitized solar cells (DSSCs), the photoelectrical conversion efficiency of TiO_2 nanotubes is much higher than that of nanorods, and the highest value (3.26%) is located at the etching temperature of 140 ℃. It could be deduced that the increased specific surface area and length shortening of the nanotube play the positive and negative effect on the photoelectrical property, respectively. Furthermore, the calcination effect on the structure and photovoltaic property of TiO_2 nanotubes is also carried out. However, the fracture and aggregation of nanotubes could be observed after heating treatment, which therefore increase the difficulty of photo-induced carriers in directional transfer and also reduce the photoelectrical activity.

Key words: TiO_2 nanotube; etching treatment; growth mechanism; photoelectric property
CLC number: TN36 **Document code**: A **DOI**: 10.3788/fgxb20194004.0459

TiO_2 纳米管刻蚀生长机理及其光电性能

孙 琼[1,2*], 游 迪[1], 臧 韬[1], 吴松浩[1], 洪 永[1], 董立峰[1]

(1. 青岛科技大学 材料科学与工程学院, 山东 青岛 266042;
2. 福州大学 能源与环境光催化国家重点实验室, 福建 福州 350116)

摘要: 采用盐酸将有序排列的 TiO_2 纳米棒刻蚀成纳米管,并推测了生长机理。刻蚀过程中,凹陷沿棒生长方向自上而下由内而外产生,最终形成管式结构。大量纳米线围绕成具有方形空心截面的纳米管,高温下将完全分裂。TiO_2 纳米管的光电转换效率远高于纳米棒,最高值(3.26%)出现在 140 ℃刻蚀温度。纳米管比表面积增加和长度缩短分别对光电性能起到正反两方面作用。此外,煅烧导致纳米管断裂和聚集,光生载流子定向转移的难度增加,光电转换效率降低。

关 键 词: TiO_2 纳米管; 刻蚀; 生长机理; 光电性能

收稿日期: 2018-05-25; **修订日期**: 2018-09-10
基金项目: 国家自然科学基金青年基金(51402161); 福州大学能源与环境光催化国家重点实验室开放课题(SKLPEE-KF201707)资助项目
Supported by National Natural Science Foundation of China(51402161); Open Project Program of State Key Laboratory of Photocatalysis on Energy and Environment, Fuzhou University(SKLPEE-KF201707)

1 Introduction

As one of the promising alternatives to the conventional silicon solar cell, dye-sensitized solar cells (DSSCs) have attracted immense interests in scientific and industrial research owing to their low material and production cost and high photoelectrical conversion efficiency[1-3]. Some n-type semiconductor metal oxides such as TiO_2, ZnO[4-6], Fe_2O_3[7] and WO_3[8] are suitable for the photoanode materials. Due to the strong affinity to dye molecules and high chemical stability, TiO_2 based DSSCs have attracted the most attention and shown excellent performance in photoelectrical conversion[9]. As a result, special shaped TiO_2 nano-materials such as nanosphere, nanorod, nanotube, nanowire, and nanosheet, *etc*. have been already prepared from various ways[10-14].

Compared to other counterparts, the one-dimensional (1-D) TiO_2 with directional arrangement such as nanotube, nanorod or nanowire arrays owning precisely oriented nature and excellent electron percolation pathways can offer a direct electrical channel of photo-generated charge that suitable for electron transfer, thus has attracted plenty of attention and been widely employed in photoelectrochemical cells[15], photocatalytical treatments[13], as well as water-splitting reactions[16]. Among these 1-D architectures, the TiO_2 nanorod array (NRA) consist of mono-crystalline is studied firstly and mostly because of their superior chemical stability, excellent electron transport properties, structure controllability and low cost[17-19]. Various chemical techniques have been reported for preparing mono-crystallized TiO_2 NRAs, including chemical vapor deposition (CVD)[20-21], metal-organic chemical vapor deposition method(MOCVD)[22], hydrothermal method[23-24], chemical bath deposition[25], and so on. Since Liu[26] introduced a direct hydrothermal method for the growth of oriented, single-crystallized rutile TiO_2 nanorod film on FTO conductive substrates, many related studies of DSSCs have been developed focusing on this *in-situ* hydrothermal process[27]. However, owing to the relative low surface area of rutile TiO_2 NRAs, the photoelectrical conversion efficiency of DSSCs based on such photoanodes is significantly confined. Liu *et al*.[28] reported an anisotropic corrosion strategy for the transformation of TiO_2 nanorods into nanotubes with hydrochloric acid as the etching agent under hydrothermal condition. As a result, the surface area of received 1-D TiO_2 nanotubes was effectively enlarged. Lv *et al*.[29] reported the vertically aligned single-crystallized rutile TiO_2 NRAs with large internal surface area that prepared directly on FTO substrates by a facile two-step hydrothermal process, and a photoelectrical efficiency of 5.94% was finally achieved on the DSSC assembled with the etched TiO_2 NRAs, which was much higher than that with untreated NRAs(3%).

In this study, vertically aligned single-crystalline rutile TiO_2 nanotube films with large surface area were prepared from a modified two-step hydrothermal process, using concentrated hydrochloric acid as the etching agent. The perovskite $CsSnI_{2.95}F_{0.05}$ was synthesized and utilized as the solid electrolyte for the fabrication of the all-solid-state dye-sensitized solar cell. Then the effects of the etching and calcination treatment on the photoelectric conversion efficiency were discussed. In addition, the growth mechanism of the TiO_2 nanotube was also assumed, and the effect of different additives during the second hydrothermal process was also clarified.

2 Experiment

2.1 Synthesis of TiO_2 Nanotubes

The TiO_2 nanorod array films were prepared directly on transparent conductive fluorine-doped tin oxide (FTO) substrates by a modified hydrothermal method[26]. In a typical synthesis process, 15 mL of deionized (DI) water was mixed with 15 mL of concentrated hydrochloric acid (36.0% – 38.0%) in a Teflon-lined stainless steel autoclave. The mixture was stirred for 10 min under ambient conditions, and then 0.6 mL of butyl titanate was added to the mixed solution and stirred for another 10 min. A piece of FTO substrate (4 cm × 2.5 cm) was placed at an angle against the wall of the Teflon-liner with the conducting side facing down. Hydrothermal synthesis was

conducted at 150 ℃ for 4 h in an oven, and the autoclave was then cooled to room temperature in air.

The TiO_2 nanotubes were synthesized by a second hydrothermal process with hydrochloric acid as the etching agent[29]. The as-prepared film on FTO substrate was immersed into the autoclave containing 15 mL DI water and 15 mL concentrated hydrochloric acid (36.0% – 38.0%). The chemical etching reaction was conducted by hydrothermal method at 120 – 200 ℃ for 3 h. The received sample was rinsed with DI water extensively and dried in air. Moreover, the sintering treatment was set at 200 – 500 ℃ for 3 h, respectively.

2.2 Characterization

Morphological information of the samples was observed by field-emission scanning electron microscope (FESEM, JEOL JSM-6700F) and transmission electron microscope (TEM, JEOL JEM-2100). The crystal structure was examined by X-ray diffraction (XRD, Rigaku, D/MAX-2500/PC) using Cu Kα as X-ray radiation source (40 kV, 100 mA) and scanning from 20° to 90°.

2.3 Fabrication of DSSCs

DSSCs were fabricated with the TiO_2 film grown on FTO as the photoanode. The photoanode was immersed in a 0.3 mmol/L ethanol solution of cis-bis (isothiocyanato) bis(2,2′-bipyridyl-4,4′-dicarboxylato)-ruthenium (Ⅱ) bis-tetrabutylammo-nium dye (N719) for 12 h in the dark. After the adsorption equilibrium reached, the samples were taken out and rinsed with deionized water to remove surface dissociative dye. The platinum-coated FTO substrate was used as the counter electrode, which was prepared by thermal decomposition of H_2PtC_{l6} solution in isopropanol sintered at 400 ℃ for 20 min. The perovskite $CsSnI_{2.95}F_{0.05}$ dissolved in N,N-dimethylformamide (DMF) was filled into the space between the two electrodes as the electrolyte, which was prepared according to our previous report[30]. Until the DMF was totally evaporated at room temperature, the all-solid-state DSSC was ready.

2.4 Photovoltaic Measurement

Photocurrent-voltage (*J-V*) curves of DSSCs were tested on a CHI760D electrochemical working station. The illumination was provided by a solar simulator (150 W, Newport 96000) with air mass 1.5 global filter (AM 1.5G, Newport 81094), which was calibrated by a high power thermal detector (Physcience Opto-Electronics, Beijing, LP-3A). The light power density was set as 100 mW/cm^2 to simulate the sun illumination. The active surface area of cells in our test is around 0.5 cm^2 with circular shading mask. For each sample, the best result among nine parallel sample cells was recorded.

3 Results and Discussion

3.1 Effect of Etching Temperature

The typical FESEM images of the TiO_2 nanorods and nanotubes are shown in Fig. 1. It can be seen that densely aligned TiO_2 nanorod grew uniformly on the FTO substrate after 4 h hydrothermal reaction at 150 ℃ (Fig. 1(a)). The nanorods were tetragonal in shape with square top facets and little space exists between adjacent TiO_2 nanorods. When etched at 120 ℃ for 3 h, the top of the nanorods began to cave and became rough (Fig. 1(b)). Many bulges appeared at the top of each individual TiO_2 nanorod and apparent space between adjacent bulges can be observed. While the etching temperature increased to 140 ℃, the nanorods converted thoroughly into tubular structure with square cross section (Fig. 1(c)). Furthermore, it can be found that the tube wall was assembled by a mass of surrounded fine TiO_2 nanowires. While etched at 180 ℃, the wall of nanotubes became thinner and some of TiO_2 nanotubes were even teared into independent nanowires (Fig. 1(d)). After etching at 200 ℃, most of the nanotubes were totally destroyed and gathered into nanowire clusters (Fig. 1(e)). The effect of etching temperature on the length of nanotubes was also studied and summarized in Fig. 1(f). From 120 ℃ to 200 ℃, the average lengths decreased significantly from 1.59 μm to 1.00 μm, which were all much lower than that of untreated TiO_2 nanorods (1.81 μm). Moreover, from the FESEM images, the nanotube wall also became thinner and thinner with the etching temperatures. As a result, the etching step greatly destroyed the solid TiO_2 nanorods,

which happened from the top down and inside out by the driving force. Meanwhile, the nanorods also broke from the centre of the top during the corrosion process.

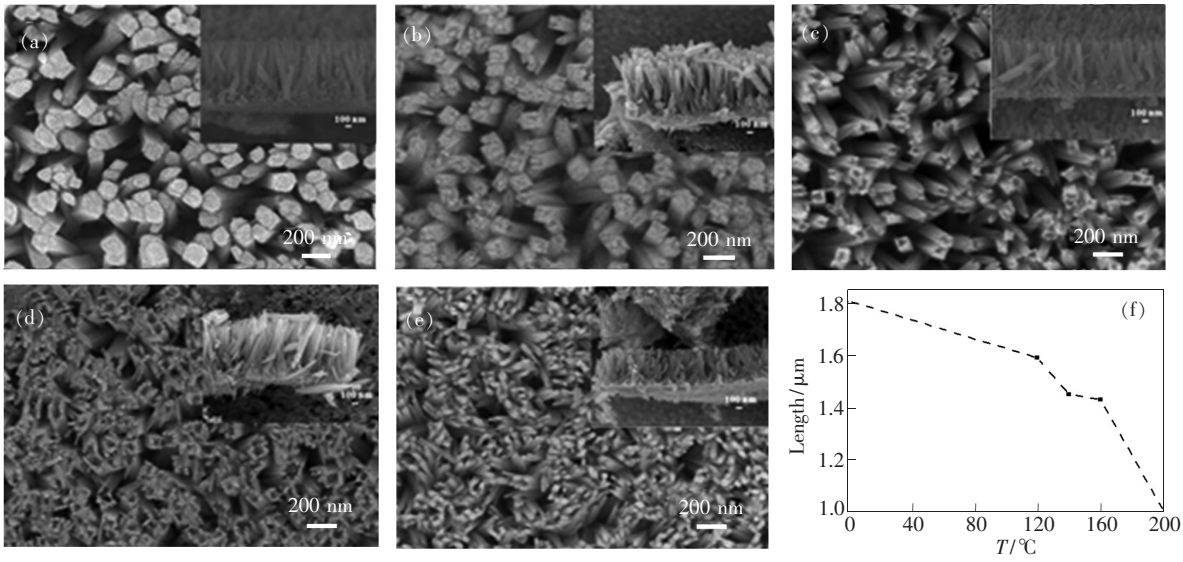

Fig. 1 FESEM images of untreated TiO_2 nanorods(a) and TiO_2 nanotubes etched at 120 ℃(b), 140 ℃(c), 180 ℃(d) and 200 ℃(e), respectively. (f) Average length of TiO_2 nanorods and nanotubes etched at different temperatures.

In order to clarify the effect of hydrochloric acid, the second hydrothermal process(140 ℃, 3 h) was also carried out in the presence of NaOH aqueous solution(pH = 12) or pure deionized water, respectively. As a result, both of the products still kept in nanorod structures(Fig. 2(a) and (b)), proving the etching effect of hydrochloric acid on TiO_2 nanorods during the hydrothermal reaction.

Fig. 3 showed the XRD patterns of the TiO_2 nanotubes etched at different temperatures, as well as the untreated TiO_2 nanorods for comparison. It confirmed that either TiO_2 nanorods or nanotubes were both formed in rutile phase(PDF No. 21-1276), meaning no phase transformation occurred during the etching process. Compared with the polycrystalline rutile TiO_2, the (002) diffraction peaks of TiO_2 nanorod and nanotube arrays were significantly enhanced, while some diffraction peaks such as (110), (111) and (211) were absent. According to the references[26,29] for the preparation of TiO_2 nanorod and nanotube arrays and the HRTEM images (Fig. 4(c) and (d), vide infra), the received TiO_2 nanorod or nanotube arrays were both formed in mono-crystal rutile phase and grown along [001] direction with the growth axis parallel to the substrate

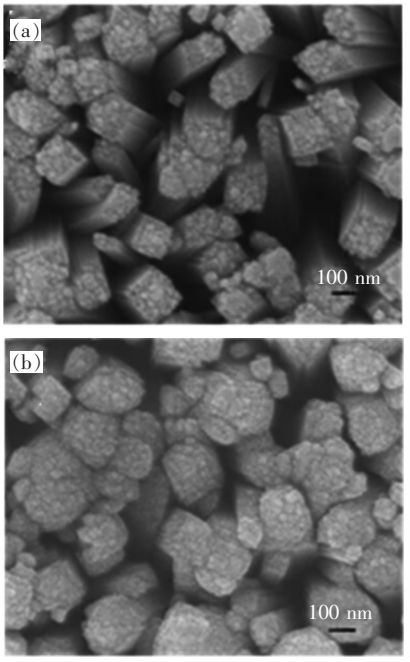

Fig. 2 FESEM images of TiO_2 obtained from the second hydrothermal process in NaOH aqueous solution (pH = 12)(a) and deionized water(b), respectively.

surface normal, which means that the nanorods and nanotubes are not only aligned but also monocrystalline throughout their length. As a result, the diffraction peaks of TiO_2 arrays in this research are not well corresponded with the standard XRD pattern of rutile TiO_2(PDF No. 21-1276). In addition, the intensity

of (101) diffraction peak kept nearly unchanged, while the (002) diffraction peak weakened gradually with etching temperatures, which indicated that the growth along [001] direction was destroyed by etching treatment. According to our previous work[30], in the first hydrothermal step, TiO_2 nanorods formed preferentially along [001] direction with the growth axis perpendicular to the FTO substrates. From the characterization of FESEM and XRD, it could be proved that the destruction to the nanorods by hydrochloric acid also occurred from [001] direction, and finally produced hollow and shortened nanotubes.

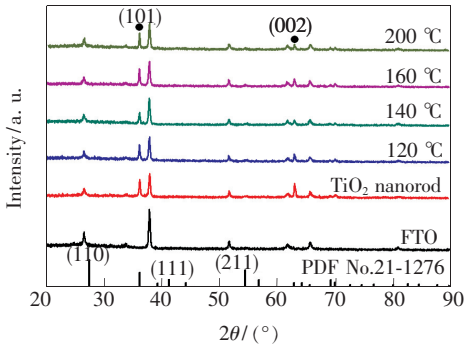

Fig. 3　XRD patterns of TiO_2 nanorods and nanotubes etched at different temperatures

In addition, transmission electron microscope (TEM) and high-resolution TEM (HRTEM) were also carried out. Compared to TiO_2 nanorods (Fig. 4(a)), a V-shaped hollow top appeared in TiO_2 nanotube (Fig. 4(b)). It is confirmed that the nanotube owns a much higher specific surface area than that of the corresponding nanorod precursor. From HRTEM images, two orthogonal interplanar spacings of (0.32 ± 0.01) nm and (0.29 ± 0.01) nm could be found both from the nanorod and nanotube (Fig. 4(c) and (d)), corresponding to the *d*-spacing of the rutile (110) and (001) planes respectively, which further proved that the long axis growth direction was along [001] direction. From the report, the growth rate of different crystal faces in rutile TiO_2 nanorods follows the order: (001) > (101) > (100) > (110)[31]. When the nanorods were treated by hydrochloric acid during the second hydrothermal process, the (001) planes should be thus preferentially etched[32]. The decreasing concentration of hydrochloric acid along the [001] direction in the confined space of the TiO_2 nanotube and the increased exposure to corrosion for the previously eroded side wall induced the formation of V-shaped structure[28].

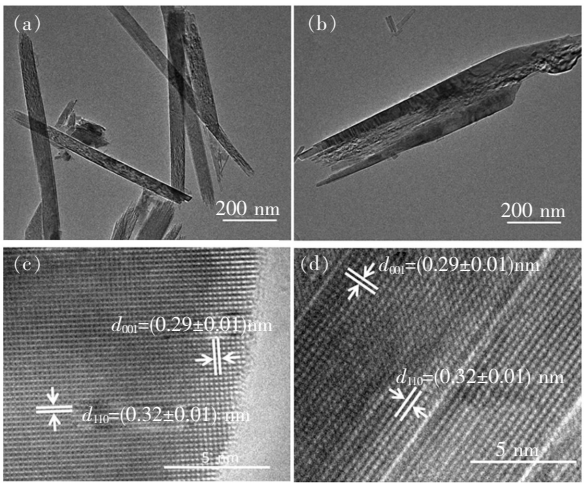

Fig. 4　TEM and HRTEM images of TiO_2 nanorods (a, c) and nanotubes (b, d)

Fig. 5 displays the photocurrent density-voltage curves of the dye sensitized solar cells assembled with TiO_2 nanotubes etched at different temperatures, and the corresponding photovoltaic parameters including open-circuit voltages (V_{OC}), short circuit current densities (J_{SC}), conversion efficiencies (η) and fill factors (FF) are summarized in Tab. 1. Once the nanorods were etched into nanotubes at 120 ℃ to 200 ℃, the photovoltaic property of the solar cell was improved first and then worsened, with the optimal photoelectrical conversion of 3.26% at

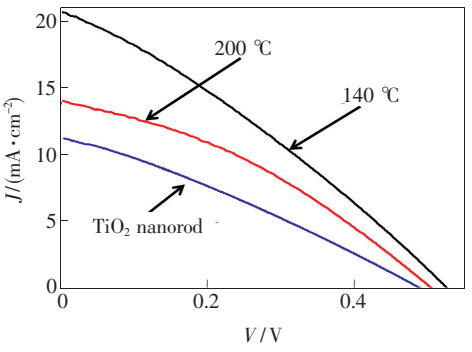

Fig. 5　Current density-potential (J-V) curves of the DSSCs assembled with TiO_2 nanorods and nanotubes etched at 140 ℃ and 200 ℃ under the irradiation of solar simulator

140 ℃. When the configuration of nanotube formed in TiO_2, the highly expanded specific surface area was beneficial for the adsorption of dye and absorption of incident photons, and also supplied more pathways for the photo-induced charge transfer. Therefore, a solar cell with modified photoelectrical performance was obtained. However, the etching treatment would simultaneously destruct the orientated growth of TiO_2 arrays and thin the photoanode, especially at high temperature, which thus decreased the dye adsorption, the absorption to the incident irradiation, and also the yield of the photoelectron-hole pairs. Furthermore, the adhesion between the film and FTO substrate became weak as the growth destruction of TiO_2, resulting in a higher resistance for the transfer of photogenerated carriers. In summary, the etching treatment to TiO_2 nanorod would make a positive contribution to the photoelectrical activity within a certain temperature range. When HCl was absent during the second hydrothermal process, it has been proved that the etching process couldn't occur and thus the photoelectrical conversion kept nearly unchanged (1.65%) to TiO_2 nanorod (1.63%). Moreover, the addition of NaOH in the second hydrothermal process would greatly reduce the photoelectrical conversion (0.38%). According to our precious work[33], this decline is because more hydroxyl groups on the surface of TiO_2 can be produced during the alkaline hydrothermal treatment than the acidic condition, which can change the interface structures between TiO_2 and dye molecules, and finally decrease the photoelectrical activity.

Tab. 1 Photovoltaic parameters of DSSCs with TiO_2 nanorods and nanotubes etched at different temperatures

T/℃	J_{SC}/(mA·cm^{-2})	V_{OC}/V	FF	η/%
Nanorod	11.27	0.50	0.29	1.63
120	17.83	0.53	0.27	2.59
140	20.70	0.53	0.29	3.26
140*	16.62	0.51	0.19	1.65
140**	2.36	0.61	0.26	0.38
160	19.32	0.58	0.29	3.20
180	19.80	0.57	0.28	3.19
200	14.02	0.51	0.35	2.48

* and **: The solar cells were fabricated with the nanorods that treated with deionized water and NaOH aqueous solution (pH = 12) during the second hydrothermal process, respectively.

3.2 Effect of Calcination Treatment

The calcination treatment of TiO_2 was usually used to improve the crystallinity degree and also photoactivity in many reports[30,34]. In the following discussion, unless noted otherwise, the etching process was carried out at 140 ℃ for 3 h. When higher than 500 ℃, the FTO substrate would melt and bend, thus the highest temperature was set at 500 ℃. As the calcination temperature increased from 200 ℃ to 500 ℃, in FESEM images(Fig. 6), TiO_2 nanotubes still attached to FTO substrate. However, the fracture of nanotubes could be observed from embedded figures, which resulted in the decreased average length. Meanwhile, the hollow part

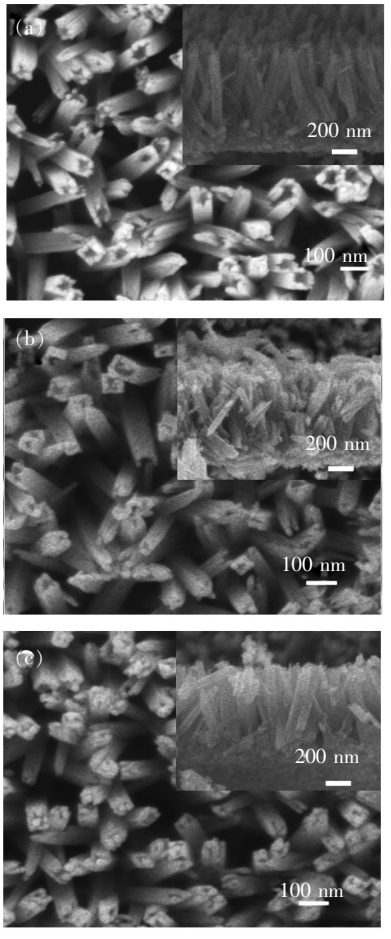

Fig. 6 FESEM images of the top and cross-sectional views of TiO_2 nanotubes sintered at 200 ℃(a), 400 ℃(b) and 500 ℃(c) for 3 h.

in nanotube became much smaller than that of unsintered sample, indicating that the surrounding nanowires tended to aggregating together during the heating process.

According to XRD patterns (Fig. 7), the diffraction peaks of sintered samples were still indexed to rutile TiO_2 (PDF No. 21-1276). Furthermore, the intensity of all peaks kept nearly the same with the unsintered sample, which proved that although the tubular structure shrunken at high temperature, the crystallinity formed from the epitaxial growth on FTO during the hydrothermal process was relatively stable.

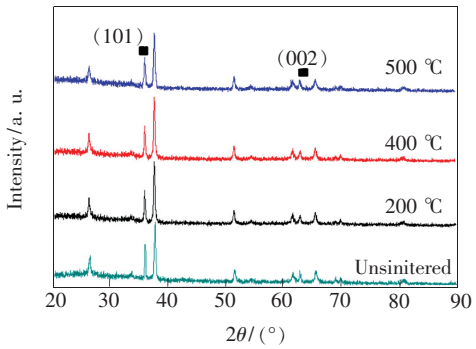

Fig. 7　XRD patterns of TiO_2 nanotubes sintered at different temperatures. From bottom to top: unsintered, sintered at 200, 400, 500 ℃, respectively.

The photovoltaic properties of the solar cells containing sintered TiO_2 nanotubes were tested and summarized in Tab. 2. After the sintering treatment, the values of J_{SC} and η both decreased rapidly compared to the unsintered sample. According to the morphology and crystal characterizations in Fig. 6 and 7, the most obvious change resulted from the sintering treatment was the break and aggregation of the nanotubes, which both raised the difficulty of the directional transfer of photo-generated electrons and finally decreased the photoelectrical conversion efficiencies.

Tab. 2　Photovoltaic performance of DSSCs fabricated with sintered TiO_2 nanotubes

T/℃	J_{SC}/(mA · cm^{-2})	V_{OC}/V	FF	η/%
Unsintered	20.70	0.53	0.29	3.26
200	10.13	0.62	0.26	1.64
300	9.51	0.61	0.26	1.52
400	6.05	0.64	0.37	1.44
500	6.01	0.65	0.33	1.29

4　Conclusion

In this research, the monocrystalline rutile TiO_2 nanotube arrays on FTO substrate were prepared with hydrochloric acid as the etching agent at different temperature. The morphology and crystal structure were tested by FESEM, XRD and HRTEM, and their effect on the photoelectrical performance of the DSSC that fabricated with the TiO_2 nanotube was also discussed. During the etching process, the transformation of the nanorod into nanotube gradually occurred from top down and inside out, accompanying with the shortening of the length and thinner of the nanotube wall simultaneously, while the higher the etching temperature, the clearer the nanotube structure. However, when etched at high temperature (over 200 ℃), the nanowires that surrounded connected to form the nanotubes were teared into independent ones. The enhanced surface area of the nanotube that generated from the etching treatment would contribute to the improvement of the photovoltaic property of the assembled DSSC, while the length shortening of the arrays was not favorable. As a result, the TiO_2 nanotube with the best performance in DSSC (η was 3.26%) was prepared at 140 ℃. In addition, the calcination effect on the structure and photoelectrical activity of TiO_2 nanotube was also studied. Unfortunately, both the broken and agglomeration of TiO_2 nanotubes occurred during the heating process, which thus dramatically decreased the photoelectrical conversion efficiency of the assembled DSSC.

References:

[1] O'REGAN B, GRÄTZEL M. A low-cost, high-efficiency solar cell based on dye-sensitized colloidal TiO_2 films [J]. *Nature*, 1991, 353(6346): 737-740.

[2] YELLA A, LEE H W, TSAO H N, *et al.*. Porphyrin-sensitized solar cells with cobalt (Ⅱ/Ⅲ)-based redox electrolyte

exceed 12 percent efficiency [J]. *Science*, 2011,334(6056):629-634.

[3] XIN X K,HE M,HAN W,*et al*.. Low-cost copper zinc tin sulfide counter electrodes for high-efficiency dye-sensitized solar cells [J]. *Angew. Chem. Int. Ed. Engl.*, 2011,50(49):11739-11742.

[4] 赵宇涵,李雪,关海艳,等. 快速热退火处理 ZnO 电子传输层对聚合物太阳能电池性能的改善 [J]. 发光学报, 2017,38(8):1063-1068.
ZHAO Y H,LI X,GUAN H Y,*et al*.. Enhanced performance of polymer solar cells using rapid thermal annealing treated ZnO electron transporting layer [J]. *Chin. J. Lumin.*, 2017,38(8):1063-1068. (in Chinese)

[5] KIM J H,KIM K P,KIM D H,*et al*.. Electrospun ZnO nanofibers as a photoelectrode in dye-sensitized solar cells [J]. *J. Nanosci. Nanotechnol.*, 2015,15(3):2346-2350.

[6] CHEN L Y,YIN Y T. Hierarchically assembled ZnO nanoparticles on high diffusion coefficient ZnO nanowire arrays for high efficiency dye-sensitized solar cells [J]. *Nanoscale*, 2013,5(5):1777-1780.

[7] MANIKANDAN A,SARAVANAN A,ANTONY S A,*et al*.. One-pot low temperature synthesis and characterization studies of nanocrystalline α-Fe_2O_3 based dye sensitized solar cells [J]. *J. Nanosci. Nanotechnol.*, 2015,15(6):4358-4366.

[8] ZHENG H D,TACHIBANA Y,KALANTAR-ZADEH K. Dye-sensitized solar cells based on WO_3 [J]. *Langmuir*, 2010, 26(24):19148-19152.

[9] 靳闪闪,禹益善,郝洪顺,等. $SrSnO_3$:Sm^{3+}/TiO_2 复合光阳极的制备及其光电性能 [J]. 发光学报, 2016,37(7): 786-792.
JIN S S,YU Y S,HAO H S,*et al*.. Preparation and photoelectric performance of $SrSnO_3$:Sm^{3+}/TiO_2 composite photoanode [J]. *Chin. J. Lumin.*, 2016,37(7):786-792. (in Chinese)

[10] YANG H G,ZENG H C. Preparation of hollow anatase TiO_2 nanospheres *via* Ostwald ripening [J]. *J. Phys. Chem.* B, 2004,108(11):3492-3495.

[11] 孙琼,孙先淼,李阳,等. 具有阵列-簇双层结构的 TiO_2 纳米棒的光电性能 [J]. 发光学报, 2013,34(1):61-65.
SUN Q,SUN X M,LI Y,*et al*.. Photoelectrical properties of TiO_2 nanorods with an array-cluster double-layered structure [J]. *Chin. J. Lumin.*, 2013,34(1):61-65. (in Chinese)

[12] SHANKAR K,MOR G K,PRAKASAM H E,*et al*.. Highly-ordered TiO_2 nanotube arrays up to 220 μm in length:use in water photoelectrolysis and dye-sensitized solar cells [J]. *Nanotechnology*, 2007,18(6):065707-1-11.

[13] WANG G M,WANG H Y,LING Y C,*et al*.. Hydrogen-treated TiO_2 nanowire arrays for photoelectrochemical water splitting [J]. *Nano Lett.*, 2011,11(7):3026-3033.

[14] CHEN J S,TAN Y L,LI C M,*et al*.. Constructing hierarchical spheres from large ultrathin anatase TiO_2 nanosheets with nearly 100% exposed (001) facets for fast reversible lithium storage [J]. *J. Am. Chem. Soc.*, 2010,132(17): 6124-6130.

[15] WU Z B,DONG F,ZHAO W R,*et al*.. The fabrication and characterization of novel carbon doped TiO_2 nanotubes, nanowires and nanorods with high visible light photocatalytic activity [J]. *Nanotechnology*, 2009,20(23):235701-1-9.

[16] CAO C L,HU C G,WANG X,*et al*.. UV sensor based on TiO_2 nanorod arrays on FTO thin film [J]. *Sens. Actuators* B *Chem.*, 2011,156(1):114-119.

[17] DIEBOLD U. The surface science of titanium dioxide [J]. *Surf. Sci. Rep.*, 2003,48(5-8):53-229.

[18] BAREA E,XU X Q,GONZÁLEZ-PEDRO V,*et al*.. Origin of efficiency enhancement in Nb_2O_5 coated titanium dioxide nanorod based dye sensitized solar cells [J]. *Energy Environ. Sci.*, 2011,4(9):3414-3419.

[19] MU Q H,LI Y G,ZHANG Q H,*et al*.. Template-free formation of vertically oriented TiO_2 nanorods with uniform distribution for organics-sensing application [J]. *J. Hazard. Mater.*, 2011,188(1-3):363-368.

[20] LIU H,ZHANG Y,LI R Y,*et al*.. A facile route to synthesize titanium oxide nanowires *via* water-assisted chemical vapor deposition [J]. *J. Nanopart. Res.*, 2011,13(1):385-391.

[21] PENG X S,CHEN A C. Aligned TiO_2 nanorod arrays synthesized by oxidizing titanium with acetone [J]. *J. Mater. Chem.*, 2004,14(16):2542-2548.

[22] WU J J,YU C C. Aligned TiO_2 nanorods and nanowalls [J]. *J. Phys. Chem.* B, 2004,108(11):3377-3379.

[23] ZHOU Q,YANG X F,ZHANG S Q,*et al*.. Rutile nanowire arrays:tunable surface densities,wettability and photochemistry [J]. *J. Mater. Chem.*, 2011,21(39):15806-15812.

[24] WANG H,BAI Y S,WU Q,*et al*.. Rutile TiO_2 nano-branched arrays on FTO for dye-sensitized solar cells [J]. *Phys.*

Chem. Chem. Phys., 2011,13(15):7008-7013.

[25] BERGER T,LANA-VILLARREAL T,MONLLOR-SATOCA D,*et al.*. The electrochemistry of transparent quantum size rutile nanowire thin films prepared by one-step low temperature chemical bath deposition [J]. *Chem. Phys. Lett.*, 2007, 447(1-3):91-95.

[26] LIU B,AYDIL E S. Growth of oriented single-crystalline rutile TiO_2 nanorods on transparent conducting substrates for dye-sensitized solar cells [J]. *J. Am. Chem. Soc.*, 2009,131(11):3985-3990.

[27] LIAO W P,HSU S C,LIN W H,*et al.*. Hierarchical TiO_2 nanostructured array/P3HT hybrid solar cells with interfacial modification [J]. *J. Phys. Chem.* C, 2012,116(30):15938-15945.

[28] LIU L,QIAN J S,LI B,*et al.*. Fabrication of rutile TiO_2 tapered nanotubes with rectangular cross-sections *via* anisotropic corrosion route [J]. *Chem. Commun.*, 2010,46(14):2402-2404.

[29] LV M Q,ZHENG D J,YE M D,*et al.*. Densely aligned rutile TiO_2 nanorod arrays with high surface area for efficient dye-sensitized solar cells [J]. *Nanoscale*, 2012,4(19):5872-5879.

[30] SUN X M,SUN Q,LI Y,*et al.*. Effects of calcination treatment on the morphology,crystallinity,and photoelectric properties of all-solid-state dye-sensitized solar cells assembled by TiO_2 nanorod arrays [J]. *Phys. Chem. Chem. Phys.*, 2013, 15(42):18716-18720.

[31] KUMAR A,MADARIA A R,ZHOU C W. Growth of aligned single-crystalline rutile TiO_2 nanowires on arbitrary substrates and their application in dye-sensitized solar cells [J]. *J. Phys. Chem.* C, 2010,114(17):7787-7792.

[32] PAN H,QIAN J S,YU A,*et al.*. TiO_2 wedgy nanotubes array flims for photovoltaic enhancement [J]. *Appl. Surf. Sci.*, 2011,257(11):5059-5063.

[33] LI Y,SUN Q,MA S,*et al.*. Synthesis of TiO_2-$SrTiO_3$ hetero-structured nanorod arrays and their photoelectrical performance in all-solid-state dye-sensitized solar cells [J]. *ECS J. Solid State Sci.*, 2015,4(3):Q17-Q20.

[34] SUN Q,SUN X M,LI Y,*et al.*. Correlations between morphology and photoelectrical properties of single-crystal rutile TiO_2 nanorods [J]. *Sci. Adv. Mater.*, 2013,5(9):1221-1230.

孙琼(1983 -),女,山东青岛人,博士,副教授,硕士研究生导师,2011年于浙江大学获得博士学位,主要从事太阳能电池和光催化的研究。
E-mail: sunqiong@qust.edu.cn